Journal of Nuclear Medicine, published on July 9, 2020 as doi:10.2967/jnumed.120.243949

Simplified Quantification of ^{11}C-UCB-J PET Evaluated in a Large Human Cohort

Mika Naganawa[1], Jean-Dominique Gallezot[1], Sjoerd J. Finnema[1], David Matuskey[1,2,3], Adam Mecca[2], Nabeel B. Nabulsi[1], David Labaree[1], Jim Ropchan[1], Robert T. Malison[2], Deepak Cyril D'Souza[2], Irina Esterlis[2], Kamil Detyniecki[3], Christopher van Dyck[2], Yiyun Huang[1],Richard E. Carson[1]

[1]PET Center,Department of Radiology and Biomedical Imaging,Yale University,New Haven,CT,USA;

[2]Department of Psychiatry,Yale University,New Haven,CT,USA;

[3]Department of Neurology,Yale University,New Haven,CT,USA

Corresponding author: Mika Naganawa,Yale University,801 Howard Avenue PO Box 208048,New Haven,CT,06520-8048,United States.Phone number:203-737-5582,E-mail:mika.naganawa@yale.edu

Financial support:R01NS094253,R01AG052560,R01MH104459,Nancy Taylor Foundation

Word count:2499/2500

Running Title:SUVR of ^{11}C-UCB-J in humans

ABSTRACT

^{11}C-UCB-J is a PET tracer for synaptic vesicle glycoprotein 2A which may be a marker of synaptic density. To simplify the scan protocol, standardized uptake value ratios (SUVR) were compared to model-based binding potential (BP_{ND}) to select the optimal time window in healthy and neuropsychiatric subjects.

Methods: A total of 141 scans were acquired for 90min. Arterial blood sampling and metabolite analysis were conducted. SUVR-1 (centrum semiovale reference region) was computed for six 30-min windows and compared with 1-tissue compartment model BP_{ND}. Simulations were performed to assess the time dependency of SUVR-1.

Results: Greater correlation and less bias were observed for SUVR-1 at later time windows for all subjects. Simulations showed that the agreement between SUVR-1 and BP_{ND} is time-dependent.

Conclusion: The 60-90min period provided the best match between SUVR-1 and BP_{ND} (-1±7%), thus, a short scan is sufficient for accurate quantification of ^{11}C-UCB-J specific binding.

Key words

Synaptic vesicle protein 2A;SV2A;Positron emission tomography;SUVR;Brain imaging

INTRODUCTION

PET imaging with ^{11}C-UCB-J has enabled the visualization of the synaptic vesicle protein 2A (SV2A) *in vivo* in humans and may provide a quantitative measurement of synaptic density. SV2A imaging with ^{11}C-UCB-J revealed lower synaptic density in temporal lobe epilepsy (*1*), Alzheimer's disease (AD) (*2*), major depressive disorder (*3*), and Parkinson's disease (*4*). In humans, ^{11}C-UCB-J displayed high brain uptake and fast kinetics with excellent test-retest reproducibility (3-9%) for volume of distribution (V_T) calculated by the one-tissue compartment (1TC) model (*5*). However, quantification with the 1TC model requires arterial blood sampling and a PET scan of ≥60min. To simplify the scan protocol, we evaluated two ratios, tissue-to-plasma (TTP) and tissue-to-reference (standardized uptake value ratios, SUVR), for quantification against the gold standard parameters V_T and binding potential (BP_{ND}), respectively, in healthy subjects (HS) and neuropsychiatric subjects (NS). A previous study (*6*) showed the time window of 60-90min was the best for SUVR-1 using 10 HSs. Here, expanded on that study using a much larger cohort of HS and NS groups.

MATERIALS AND METHODS

Human Subjects

This study includes a total of 141 subjects composed of 51 HSs (M/F=33/18,age:48±17, BMI:27±5) and 90 NSs (M/F=59/31,age:42±15,BMI:28±5): 11 with Alzheimer's disease (AD), 5 with epilepsy (EP), and 75 other NSs (Supplemental Table 1). Study protocols were approved by the Yale Human Investigation Committee, the Yale-New Haven Hospital Radiation Safety Committee or the Yale Radioactive Drug Research Committee, and performed in accordance with federal guidelines and regulations of the United States for the protection of human research subjects contained in Title 45 part 46 of the Code of Federal Regulations. All subjects signed a written informed consent form. As part of the subject evaluation, magnetic resonance (MR) images were

acquired on all subjects to eliminate those with significant anatomical abnormalities not consistent with their illness and for PET image registration.

Data Acquisition

^{11}C-UCB-J was prepared as described previously (*7*). All subjects underwent 90min PET scans on the High Resolution Research Tomograph (HRRT) (Siemens Medical Solutions, Knoxville, TN) after a bolus injection of ^{11}C-UCB-J (536±192 MBq,*n*=141) over 1min. Dynamic scan data were reconstructed in 27 frames (6×0.5min,3×1min,2×2min,16×5min) with corrections for attenuation, normalization, scatter, randoms, and deadtime using the MOLAR algorithm (*8*). Motion correction was performed using measurements with the Polaris Vicra sensor (NDI Systems, Waterloo, Canada) with reflectors mounted on a swim cap worn by the subject. The metabolite-corrected arterial input function was acquired as described previously (*5*).

Image Registration and Region of Interests

After image registration between MR and an averaged PET image, 14 regional time–activity curves (TACs) were generated for the cerebral cortex (frontal, temporal, occipital, and parietal cortices, insula, and cingulum), subcortical regions (hippocampus, caudate, putamen, pallidum, thalamus, hypothalamus), cerebellum, and centrum semiovale (*2,9*) using the combined transformations from template-to-PET space (*5*).

Quantitative Analysis

The 1TC model was applied to regional TACs (90min) to estimate V_T and BP_{ND}. Centrum semiovale was used as the reference region (*1*). TTP and SUVR-1 values were computed as the ratio of the average values across frames in each time window:10-40, 20-50, 30-60, 40-70, 50-80, and 60-90min, for comparison with V_T and BP_{ND}, respectively. The optimal time window was selected by comparing percent difference (*pd*) between SUVR-1 and BP_{ND} values across the HSs and all NSs.

To assess whether the SUVR and BP_{ND} relationship was affected by demographics, age, gender, and body mass index (BMI), interactions with the *pd* between SUVR-1 and BP_{ND} were assessed with analysis of covariance (ANCOVA) in HSs.

Subsequently, the performance of the selected time window was evaluated in two specific clinical populations. In AD (*2*), the group differences in hippocampal BP_{ND} and SUVR-1 between age-matched subjects (HS:n=7 vs. AD:n=9) were assessed; the hippocampus showed the clearest group difference for ^{11}C-UCB-J (*2*). In EP (*1*), SUVR-1 and BP_{ND} were compared in the ipsilateral and contralateral hippocampus. Between-group differences were computed using *t*-test for both model-based and simplified measures.

Simulation Study

To investigate the full time dependency of SUVR-1 values, noise-free data were simulated using the estimated K_1 and k_2 values of all subjects for frontal cortex, hippocampus, and centrum semiovale. A mono-exponential clearance rate (β) of the input function (t>20min) was estimated to extrapolate the input function (β=0.0095±0.0023 1/min,n=141). TTP and SUVR-1 were computed for 45 time windows with 30-min duration, beginning at 10, 20,…, and 4500min post-injection. TTP and SUVR-1 were compared with the true V_T and BP_{ND}. In addition, these parameters were compared with their transient equilibrium (TE) values (*10*), i.e., the constant TTP and SUVR values ultimately reached following a bolus injection. The TE V_T and BP_{ND} values were computed using the estimated β and kinetic parameters as $V_T/(1-\beta/k_2)$ and $(BP_{ND}+1)(1-\beta/k_{2,REF})/(1-\beta/k_2)-1$. TTP and SUVR-1 were compared with the true and TE V_T and BP_{ND} values, respectively.

Stastical Analsis

Data were expressed as a mean and standard deviation unless otherwise indicated. *pd* between X and Y was computed as $(X/Y-1)\times 100\%$ using all regions and all subjects unless otherwise indicated. Comparisons between 2 groups were performed by *t*-test and Cohen's *d*. In ANCOVA, age and BMI were used as covariates, sex as an independent variable, and *pd* was the dependent

variable. For all statistical tests, $P \leq 0.05$ was considered statistically significant. Correlations between two outcome measures were assessed by Pearson *r* and linear regression.

RESULTS

BP_{ND} vs. SUVR-1

Table 1 shows comparisons of TTP and SUVR-1 in six time windows with V_T and BP_{ND}, respectively, derived from the 90-min scan data in HS (Figure 1). *pd*s between TTP vs. V_T and between SUVR-1 vs. BP_{ND} are listed in Table 2. TTP substantially overestimated V_T in all the time windows, with greater overestimation at later times, as transient equilibrium approached (*11*). When comparing BP_{ND} with SUVR-1, the results were quite different, with the 60-90min time window producing excellent agreement based on the regression lines, correlation coefficients, and *pd*s. Corresponding data in NS are shown in Supplemental Tables 2 and 3.

ANCOVA revealed that there were no significant effects of age, gender, and BMI on the relative difference between the SUVR-1(60-90min) and BP_{ND} in HS.

A linear regression analysis was performed in the hippocampus of HS and AD (Figure 2A) and showed excellent agreement. *pd*s between SUVR-1 and BP_{ND} in the hippocampus were 2±9% for HS and 11±9% for AD. The HS vs. AD group difference was significant using both SUVR-1 and BP_{ND} (SUVR-1:P=0.035,d=1.03,BP_{ND}:P=0.019,d=1.13). A linear regression analysis was also applied to contralateral and ipsilateral hippocampus regions of EPs (Figure 2B). *pd*s between SUVR-1 and BP_{ND} were again small, 1±7% (contralateral) and -1±8% (ipsilateral). The difference in asymmetry indices ((ipsi-contra)/(ipsi+contra)×2) was -2±6%, which was not significant (P=0.42, paired *t*-test). Bland-Altman plots are also shown in Supplemental Figure 1.

Simulation

Supplemental Figure 2 and Figure 3 demonstrate the effect of time window, plotted as the *pd* against theoretical values. Transient equilibrium was reached at 210min (centrum semiovale),

270min (frontal cortex), and 380min (hippocampus). At transient equilibrium, TTP overestimated V_T by 58% (centrum semiovale), 93% (frontal cortex), and 117% (hippocampus). At 60-90 minutes, overestimation was similar between cortex (76%) and white matter (74%) (Supplemental Figure 2) and thus, this overestimation canceled out when computing SUVR-1 (Figure 3).

DISCUSSION

The goal of this paper was to find a simple static time window for the measurements of synaptic density/SV2A with ^{11}C-UCB-J PET. Using tissue ratios (SUVR) and comparing to BP_{ND}, the best agreement was achieved in the 60-90min time window.

In general, stronger correlations of ratios (TTP and SUVR) with V_T and BP_{ND} were seen in later time windows. Note that the correlation coefficient between SUVR-1 and BP_{ND} did not improve for windows later than 40-70min. The magnitude of TTP overestimation over V_T increased with later time windows, as expected, while the magnitude of SUVR-1 underestimation over BP_{ND} decreased, due to cancellation of the errors between the target and reference regions. The best agreement between SUVR-1 and BP_{ND} was achieved in the time window of 60-90min.

We tested the 60-90min time window for the ability of SUVR-1 to distinguish hippocampal binding between AD and HS groups. Although SUVR-1 from the AD group slightly overestimated BP_{ND}, a significant group difference was maintained. We also found a good agreement between SUVR-1 and BP_{ND} in the ipsilateral and contralateral hippocampus regions in EP.

Since the *pd* between SUVR-1 and BP_{ND} reduced monotonically from the 10-40min window to the 60-90min window, we simulated a longer TAC to assess the time dependency of SUVR-1. As with many other tracers, simulation results revealed that the agreement between SUVR-1 and BP_{ND} is time-dependent and the *pd* continues to increase until transient equilibrium is achieved.

For ^{11}C-labeled radiotracers, later time windows tend to generate noisier images and SUV values due to radioactivity decay. However, brain uptake of ^{11}C-UCB-J is very high, and remains so even at 60-90min post-injection. For example, the ^{11}C-UCB-J SUV in the centrum semiovale at

60-90min is higher (1.32±0.30) than the SUV of the amyloid radiotracer ^{11}C-PIB in the cerebellum at 40-60min (0.69±0.07) (*12*), and thus provides statistically useful data.

Note that if there are differences in plasma clearance between subjects, the optimal time window for SUVR may shift, an effect that is handled accurately by kinetic modeling. This is the motivation for the very large cohort and diverse NS subjects used in this study. However, a larger cohort in a specific patient group would be useful for full validation. Also, while modeling requires longer scan times, it has the advantages of reducing intersubject variability, as well as providing K_1 or R_1 (tracer delivery) information, which can be a useful secondary outcome measure (*2*).

CONCLUSIONS

Based on a large cohort of HS and NS, we found that the scan period of 60-90min post-injection provided the best agreement between SUVR-1 and BP_{ND} for ^{11}C-UCB-J PET. This relationship was not affected by age, gender, or BMI. Therefore, simplified analysis with SUVR can be used for quantification of ^{11}C-UCB-J PET imaging data.

DISCLOSURE

No potential conflict of interest relevant to this article was reported.

KEY POINTS

Question: When is the optimal time window for SUVR for the SV2A tracer ^{11}C-UCB-J?

Pertinent Findings: The 60-90min period provided the best match between SUVR-1 and binding potential (-1±7%).

Implications for Patient Care: A short scan is sufficient for accurate quantification of synaptic density with ^{11}C-UCB-J.

REFERENCES

1. Finnema SJ, Nabulsi NB, Eid T, et al. Imaging synaptic density in the living human brain. *Sci Transl Med.* 2016;8:348ra396.

2. Chen MK, Mecca AP, Naganawa M, et al. Assessing synaptic density in Alzheimer disease with synaptic vesicle glycoprotein 2A positron emission tomographic imaging. *JAMA Neurol.* 2018;75:1215-1224.

3. Holmes SE, Scheinost D, Finnema SJ, et al. Lower synaptic density is associated with depression severity and network alterations. *Nat Commun.* 2019;10:1529.

4. Matuskey D, Tinaz S, Wilcox KC, et al. Synaptic changes in Parkinson disease assessed with in vivo imaging. *Ann Neurol.* 2020;87:329-338.

5. Finnema SJ, Nabulsi NB, Mercier J, et al. Kinetic evaluation and test-retest reproducibility of [(11)C]UCB-J, a novel radioligand for positron emission tomography imaging of synaptic vesicle glycoprotein 2A in humans. *J Cereb Blood Flow Metab.* 2018;38:2041-2052.

6. Koole M, van Aalst J, Devrome M, et al. Quantifying SV2A density and drug occupancy in the human brain using [(11)C]UCB-J PET imaging and subcortical white matter as reference tissue. *Eur J Nucl Med Mol Imaging.* 2019;46:396-406.

7. Nabulsi N, Mercier J, Holden D, et al. Synthesis and preclinical evaluation of 11C-UCB-J as a PET tracer for imaging the synaptic vesicle glycoprotein 2A in the brain. *J Nucl Med.* 2016:[Epub ahead of print].

8. Jin X, Mulnix T, Gallezot JD, Carson RE. Evaluation of motion correction methods in human brain PET imaging--a simulation study based on human motion data. *Med Phys.* 2013;40:102503.

9. Rossano S, Toyonaga T, Finnema SJ, et al. Assessment of a white matter reference region for (11)C-UCB-J PET quantification. *J Cereb Blood Flow Metab.* 2019:[Epub ahead of print].

10. Carson RE. PET physiological measurements using constant infusion. *Nucl Med Biol.* 2000;27:657-660.

11. Carson RE, Channing MA, Blasberg RG, et al. Comparison of bolus and infusion methods for receptor quantitation: application to [18F]cyclofoxy and positron emission tomography. *J Cereb Blood Flow Metab.* 1993;13:24-42.

12. Price JC, Klunk WE, Lopresti BJ, et al. Kinetic modeling of amyloid binding in humans using PET imaging and Pittsburgh Compound-B. *J Cereb Blood Flow Metab.* 2005;25:1528-1547.

Figures

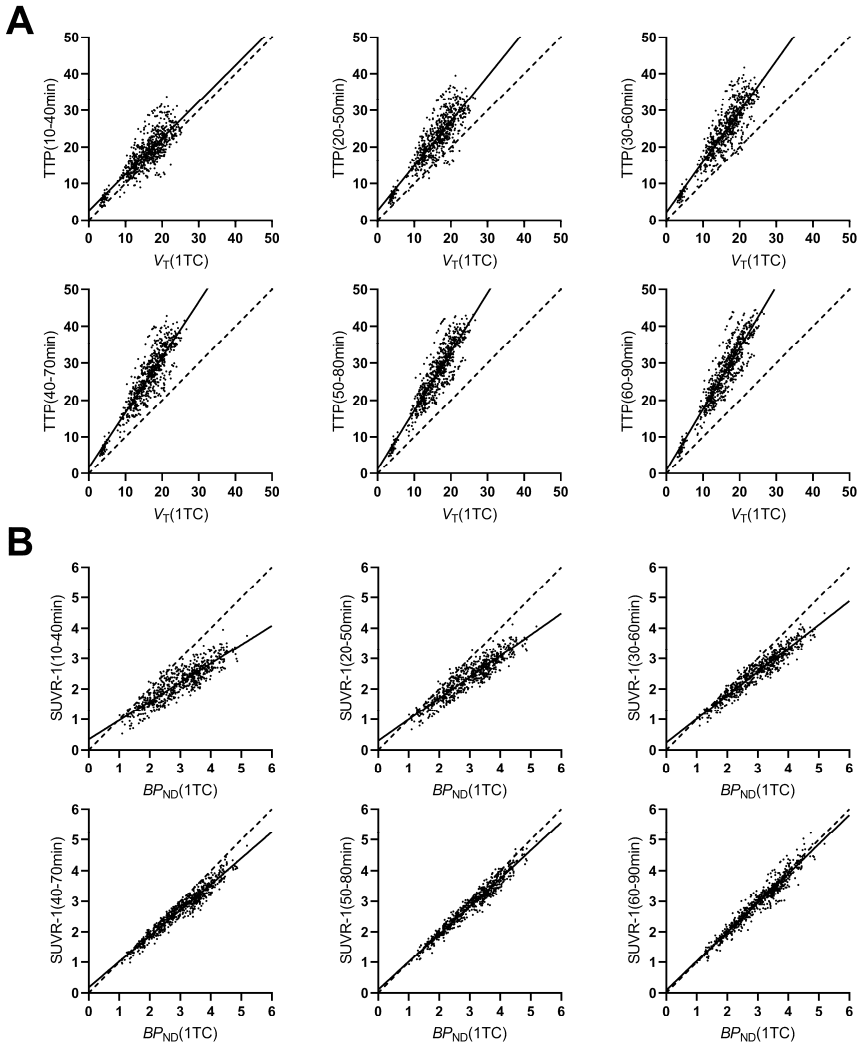

Figure 1:Scatter plots of TTP vs. V_T(90min) (A) and of SUVR-1 vs. BP_{ND}(90min) (B) with regression analysis across all regions in healthy subjects (n=51) The y axis labels define the time period for ratio calculation. See Table 1 for regression results.

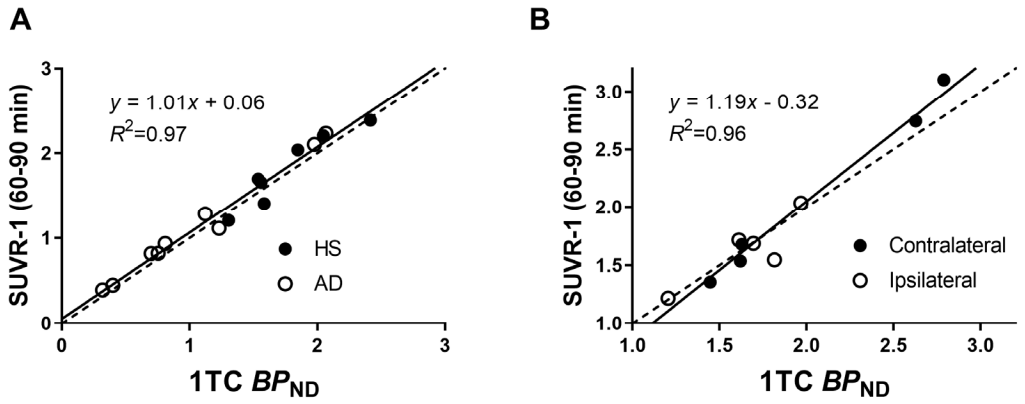

Figure 2:Scatter plots between 1TC BP_{ND} and SUVR-1 values in (A) the hippocampus of HSs and ADs and (B) contralateral and ipsilateral hippocampus of EPs.

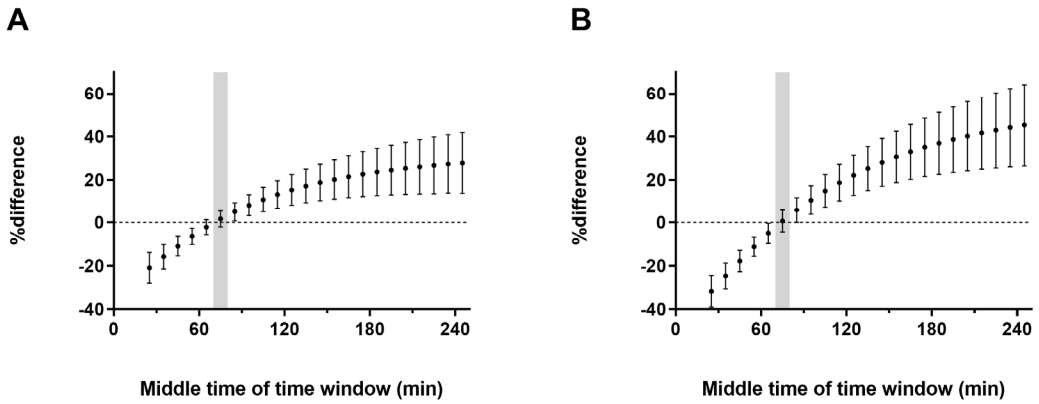

Figure 3:Mean±SD of %difference between SUVR-1 and BP_{ND} values in (A) frontal cortex and (B) hippocampus. The 60-90min time window is marked in gray.

Table 1.Linear correlations and regression analyses of TTP vs. V_T(90min) and SUVR-1 vs. BP_{ND}(90min) in healthy subjects (n=51) across all regions

Time window for TTP and SUVR-1	x=V_T,y=TTP			x=BP_{ND},y=SUVR-1		
	Slope	Intercept	R^2	Slope	Intercept	R^2
10-40min	0.99	2.57	0.71	0.62	0.35	0.79
20-50min	1.22	2.63	0.75	0.70	0.30	0.86
30-60min	1.38	2.15	0.79	0.77	0.24	0.92
40-70min	1.50	1.63	0.82	0.84	0.18	0.95
50-80min	1.59	1.22	0.84	0.91	0.11	0.96
60-90min	1.66	0.92	0.86	0.95	0.09	0.94

Table 2. %difference of TTP vs. V_T(90min) and SUVR-1 vs. BP_{ND}(90min) in healthy subjects (n=51)

Parameter	Regions	10-40min	20-50min	30-60min	40-70min	50-80min	60-90min
TTP vs. V_T(90min)	Cerebral cortex	12±19	36±21	49±21	59±21	66±21	72±21
	Subcortical	19±21	42±22	54±22	62±21	68±21	72±21
	Cerebellum	26±18	48±20	59±20	67±20	72±20	77±21
	Centrum semiovale	43±20	63±21	69±20	72±20	74±19	75±20
	Whole brain	18±21	41±22	54±22	62±21	68±21	73±21
SUVR-1 vs. BP_{ND}(90min)	Cerebral cortex	-28±8	-22±7	-16±6	-10±5	-6±5	-2±6
	Subcortical	-24±13	-18±11	-13±8	-8±6	-5±6	-2±7
	Cerebellum	-17±8	-13±6	-9±4	-5±4	-1±5	2±7
	Whole brain	-25±11	-19±9	-14±7	-9±6	-5±6	-1±7

Data are mean±SD over all subjects and all regions for each category.

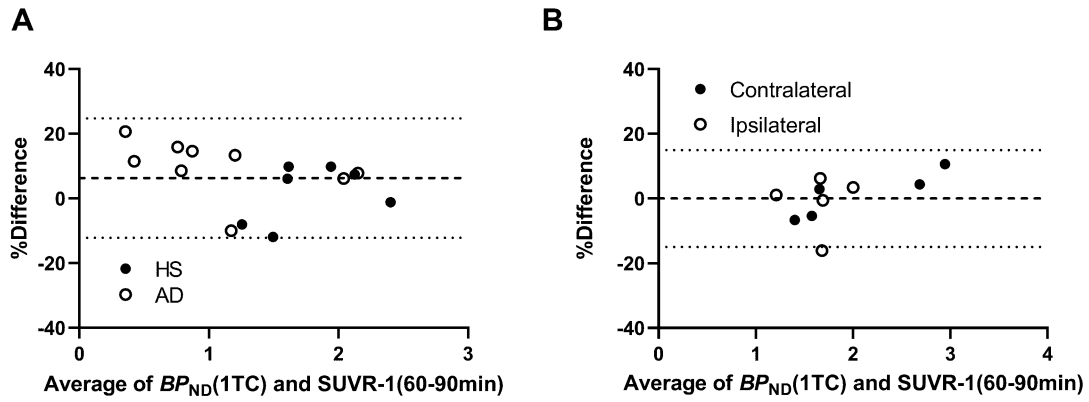

Supplemental Figure 1: Bland-Altman plots between 1TC BP_{ND} and SUVR-1 values in (A) the hippocampus of HSs and ADs and (B) contralateral and ipsilateral hippocampus of EPs.

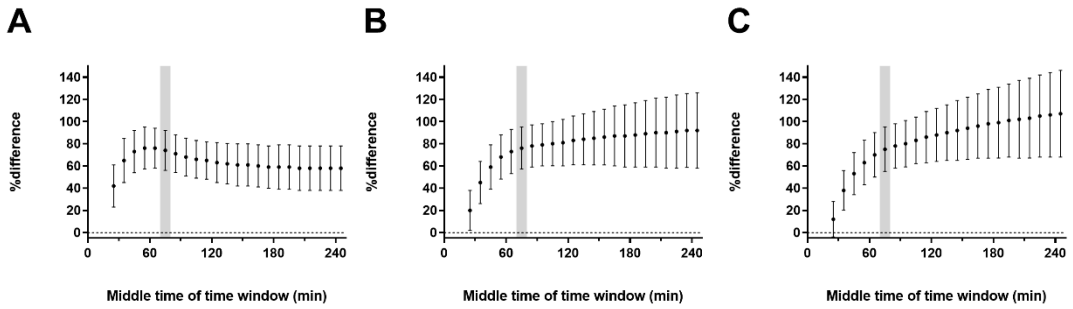

Supplemental Figure 2: Mean±SD of %difference between TTP and V_T values in (A) centrum semiovale, (B) frontal cortex, and (C) hippocampus. The 60-90 min time window is marked in gray.

Supplemental Table 1: Demographics of neuropsychiatric subjects.

Diagnosis	Number
Alzheimer's disease (*2*)	11
Bipolar	1
Cannabis dependence	9
Cocaine dependence	14
Epilepsy	5
Major Depressive Disorder (*3*)	26
Parkinson's disease (*4*)	2
PTSD	10
Schizophrenia	12
Healthy (*1-5*)	51

The references show the data that have been published elsewhere.

Supplemental Table 2: Comparisons between TTP and V_T(90 min) and SUVR-1 and BP_{ND}(90 min) in neuropsychiatric subjects (13 regions per subject, n = 90).

Time window for TTP and SUVR-1	$x = V_T$, y = TTP			$x = BP_{ND}$, y = SUVR-1		
	Slope	Intercept	R^2	Slope	Intercept	R^2
10-40 min	1.04	2.20	0.71	0.64	0.39	0.81
20-50 min	1.32	1.84	0.75	0.72	0.29	0.88
30-60 min	1.49	1.32	0.78	0.79	0.24	0.93
40-70 min	1.61	0.84	0.80	0.85	0.19	0.94
50-80 min	1.70	0.47	0.81	0.91	0.13	0.93
60-90 min	1.78	0.16	0.81	0.96	0.06	0.93

Supplemental Table 3. %difference of TTP vs. V_T(90 min) and SUVR-1 vs. BP_{ND}(90 min) in neuropsychiatric subjects (n = 90)

Parameter	Regions	10-40 min	20-50 min	30-60 min	40-70 min	50-80 min	60-90 min
TTP vs. V_T(90 min)	Cerebral cortex	14 ± 19	40 ± 23	54 ± 24	64 ± 25	72 ± 25	78 ± 26
	Subcortical	22 ± 22	47 ± 25	60 ± 25	68 ± 25	74 ± 26	79 ± 27
	Cerebellum	29 ± 21	53 ± 24	65 ± 25	72 ± 25	78 ± 25	82 ± 26
	Centrum semiovale	42 ± 22	65 ± 25	73 ± 25	77 ± 25	79 ± 26	81 ± 28
	Whole brain	19 ± 21	44 ± 24	58 ± 25	67 ± 25	73 ± 26	79 ± 26
SUVR-1 vs. BP_{ND}(90 min)	Cerebral cortex	-25 ± 8	-20 ± 7	-14 ± 6	-9 ± 6	-5 ± 7	-2 ± 7
	Subcortical	-19 ± 13	-15 ± 10	-11 ± 8	-7 ± 7	-4 ± 7	-1 ± 8
	Cerebellum	-12 ± 8	-10 ± 6	-7 ± 5	-4 ± 5	-1 ± 6	2 ± 7
	Whole brain	-22 ± 11	-17 ± 9	-12 ± 7	-8 ± 7	-4 ± 7	-1 ± 8

Data are mean ± SD over all subjects and over all regions in each catego

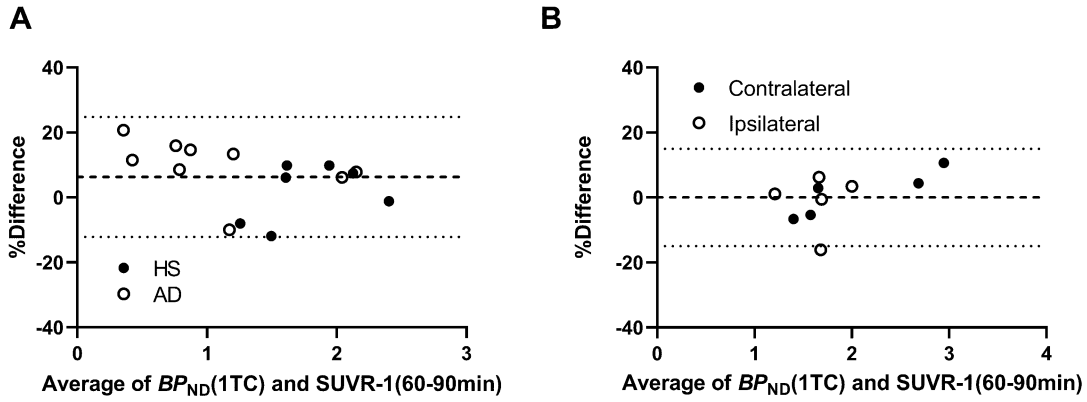

ry.